

RESEARCH

Open Access



Sustainable solidification of ferrochrome slag through geopolymerisation: a look at the effect of curing time, type of activator and liquid solid ratio

Thabo Falayi^{1,2}

Abstract

Ferrochrome (FeCr) slag was used as a precursor for the synthesis of a geopolymer. The effect of KOH concentration, liquid solid ratio (L/S), content of potassium metasilicate (KS) or potassium aluminate (KA), curing time on the unconfined compressive strength (UCS) and metal leachability of the synthesised geopolymer was investigated. A 10 M KOH and an L/S of 0.26 yielded a geopolymer with a UCS 13.0 MPa after 28 d of ambient temperature curing. A 0.125 wt KS:KOH addition yielded a geopolymer with a UCS of 14.7 MPa whilst a 1.25 wt KA:KOH addition yielded a geopolymer with a UCS of 24.5 MPa. The increase in strength was due to the formation of Calcium Silicate (Aluminate) hydrate. The aluminate activated FeCr slag geopolymer was the most competent of all geopolymers synthesised as it resulted in over 97% immobilisation of Fe, Zn, Mn, Ni and Cr. The 360-d static leachability tests for the aluminate activated geopolymer yielded a metal release rate lower than 90 mg mm⁻² of the geopolymer. The aluminate activated geopolymer also was resistant to changes in wet and dry cycles as it had a UCS reduction of 42% after 10 cycles whereas the pure FeCr slag geopolymer and the silicate activated geopolymer had a UCS reduction of 91 and 72% respectively after 10 cycles. The aluminate activated geopolymer met the minimum requirements for use as a paving brick for low traffic pavements. The study provides opportunities for sustainable use of FeCr slag with minimal environmental impact.

Keywords: Ferrochrome slag, Toxicity characteristic leaching procedure, Static leachability, Unconfined compressive strength, Wet and dry cycles

Introduction

Ferrochrome (FeCr) slag is a waste product from the carbothermic reduction of FeCr ore resulting in the production of high or low carbon FeCr alloy. It is estimated that the global annual production of FeCr alloy is between 12 and 16 Mt [1]. It also is estimated that the FeCr slag to alloy production is 1.1–1.5:1 [2]. The slag is mostly disposed of in landfills and this creates environmental problems through the utilisation of possible arable land and the leaching of metals into the environment [2].

FeCr slag is a well-known pollutant containing elevated levels of toxic elements [3, 4]. The potential release of these elements especially Cr (VI) limits the use of FeCr slag in the construction industry [5]. Exposure to Cr (VI) has been shown to cause lung cancer, pulmonary and dermatological problems [5]. FeCr slag has been classified as a non-hazardous waste in Finland [6] yet in South Africa it is classified as a hazardous waste [7]. Therefore it is imperative for more research to be explored on alternative solidification processes for FeCr slag in order to try to affect legislative change on its classification. The classification as non-hazardous of FeCr slag, may likely lead to its increased use in the construction industry, thereby leading to a reduction of volumes accumulating in landfills and fulfilling the demands of sustainable development through the use of secondary resources in the construction industry.

Correspondence: tfalayi@gmail.com

¹Department of Civil Engineering Science, University of Johannesburg, Johannesburg 2006, South Africa

²Department of Chemical Engineering, Malawi University of Science and Technology, Blantyre, Malawi



© The Author(s). 2019 **Open Access** This article is distributed under the terms of the Creative Commons Attribution 4.0 International License (<http://creativecommons.org/licenses/by/4.0/>), which permits unrestricted use, distribution, and reproduction in any medium, provided you give appropriate credit to the original author(s) and the source, provide a link to the Creative Commons license, and indicate if changes were made. The Creative Commons Public Domain Dedication waiver (<http://creativecommons.org/publicdomain/zero/1.0/>) applies to the data made available in this article, unless otherwise stated.

There are various ways in which solidification of FeCr slag can be achieved. One way is the use of Portland cement as a binder [8]. Though cement is readily available it has been shown that Cr hinders the hydration of cement leading to long term leachability problems in the hardened structures [8, 9]. FeCr slag has also been used in the construction of flexible pavements as an aggregate with reported minimal environmental contamination [10, 11]. FeCr slag has also been used with zeolites to produce bricks which can be used for construction though the study did not research on the metal leachability of the bricks [12]. Stabilisation of FeCr slag can also be achieved via alkaline activation resulting in the formation of geopolymers. Geopolymers are three dimensional amorphous or semi crystalline inorganic polymers [13]. Geopolymers have been shown to be durable, acid resistant and they have high compressive strength [13]. Geopolymers synthesised will differ from each other due to the variety of precursors and origin of the precursors [14]. This therefore calls for the research into different FeCr slag to optimise the synthesis route to suit local conditions since one size does not fit all [14]. Geopolymers have been used as concrete, mortars and grouts. The matrices of geopolymers have been shown to be capable of immobilizing toxic and nuclear wastes [14].

A few studies have been done on the alkali activation of FeCr slag [15, 16] resulting in geopolymers with the maximum 7-d unconfined compressive strength (UCS) of 20.8 MPa though there was a drop in UCS at 28 d to 13.1 MPa. These studies did not look at the immobilisation of metals with alkaline activation but looked at the fire and sulphate resistance. Environmental footprint is one of the barriers to the increased usage of FeCr slag in the construction industry.

The aim of the research was to solidify FeCr slag via geopolymerisation into useful civil engineering materials. The success of the research would then provide the opportunity to turn a waste material into a secondary resource. The effect of adding KA or KS to the original pasting solution on the geopolymerisation of FeCr slag was also investigated. The study looked at the leachability of metals from the geopolymers. The long term leachability (360 d) of the geopolymers was also studied to establish their possible environmental footprint. The synthesised geopolymers were then tested for competency against ASTM standards to gauge their usefulness in the construction industry.

Materials and methods

Materials

FeCr slag was collected from a ferrochrome smelter in South Africa. The major elements of the slag were Al, Si, K, Ca, Fe, Cr and Mg (Table 1). The FeCr slag had a pH of 8.9. In terms of Toxicity Characteristic Leaching

Table 1 XRF analysis of FeCr slag

Element	Content % wt
Na	0.230
Mg	8.581
Al	10.897
Si	47.146
P	0.0065
S	0.231
Cl	0.034
K	1.032
Ca	5.647
Ti	0.796
V	0.124
Cr	14.677
Mn	0.298
Fe	9.932
Co	0.002
Ni	0.045
Zn	0.060
Rb	0.007
Sr	0.028
Zr	0.026
Ba	0.181

Procedure (TCLP) limits, FeCr slag can be considered to be a hazardous material as the metal leachability at a pH of 4.88 was 549, 10.8, 20.5, 4.6 and 32.5 ppm for Fe, Zn, Mn, Ni and Cr, respectively: the allowable limits for these respective metals are 5, 4, 10, 0.4, and 5 ppm [17]. All chemicals used were reagent grade. KOH, potassium metasilicate (KS), Potassium aluminate (KA), Acetic acid, Sodium acetate were supplied by Rochelle Chemicals South Africa.

Equipment

The Atomic Absorption Spectroscopy (AAS, Thermo Scientific ICE 3000 Series) was used for metal analysis of leachates. The XRD (Ultima IV Rigaku) was used to analyze the mineralogical structure of FeCr slag and the geopolymers. Elemental analysis was achieved using the X-ray Fluorescence (XRF, Rigaku ZSX Primus II). The Fourier Transform Infrared Spectroscopy (FTIR, Thermo Scientific Nicolet IS10) was used to determine the bonds in the FeCr slag and the geopolymers. Particle morphology was analysed by a Scanning Electron Microscope (SEM model Tescan Vega 3 XMU).

Methods

Preliminary geopolymerisation

This was carried out to test the effect of KOH concentration and the liquid to solid ratio (L/S) on the UCS of

Table 2 Preliminary Geopolymerisation of FeCr

Sample	KOH (M)	L/S Ratio	UCS (MPa)	Standard Deviation	Sample	KOH (M)	L/S Ratio	UCS (Ma)	Standard Deviation
1	5	0.18	1.13	0.01	12	10	0.26	12.98	0.05
2	5	0.2	1.80	0.07	13	10	0.28	4.45	0.07
3	5	0.22	3.55	0.13	14	10	0.3	–	–
4	5	0.24	4.45	0.30	15	15	0.18	1.26	0.17
5	5	0.26	5.66	0.14	16	15	0.2	2.55	0.14
6	5	0.28	2.20	0.14	17	15	0.22	4.035	0.23
7	5	0.3	–	–	18	15	0.24	6.17	0.08
8	10	0.18	2.31	0.14	19	15	0.26	7.22	0.33
9	10	0.2	3.21	0.04	20	15	0.28	2.45	0.07
10	10	0.22	6.40	0.06	21	15	0.3	–	–
11	10	0.24	7.22	0.13					

the synthesised geopolymers. The UCS was used as a criterion for choosing the best curing conditions. The lumpy FeCr slag (> 9 mm) was crushed to smaller size (< 100 μm). Appropriate amounts of KOH were mixed with reverse osmosis water to make 5, 10 and 15 M solutions. Pastes were synthesised by mixing crushed FeCr slag with the respective concentration of KOH using a mixing machine [18]. The L/S was varied from 0.18 to 0.30 per different concentrations of KOH. The pastes were then poured into a 50 × 50 × 50 mm mould and allowed to harden at room temperature for 1 d. After 1-d, the hardened pastes were demoulded and cured at ambient temperature for 28 d. At the end of 28 d the UCS of the geopolymers was determined using a Cyber plus evolution compression machine at 0.25 MPa/s [19]. The laboratory mix which gave the highest UCS was

then used for subsequent tests. This geopolymer was identified as GPO.

Effect of curing time and KA/KS

From the preliminary results, 10 M KOH and a L/S of 0.26 were chosen for the determination of the effect of KA/KS and curing time on the strength of the synthesised geopolymers. The 10 M KOH and L/S of 0.26 geopolymer had the highest UCS. Appropriate amounts of KS were added respectively to the 10 M KOH solution to produce solutions with a KS:KOH ratio of 0.125 (Sample GPS1), KS:KOH 0.25 (Sample GPS2) and KS:KOH 0.5 (Sample GPS 3). The above procedure was repeated with KA where the appropriate amounts of KA were added to the 10 M KOH to produce solutions with KA:KOH ratio of 1.00 (Sample GPA1), KA:KOH 1.25

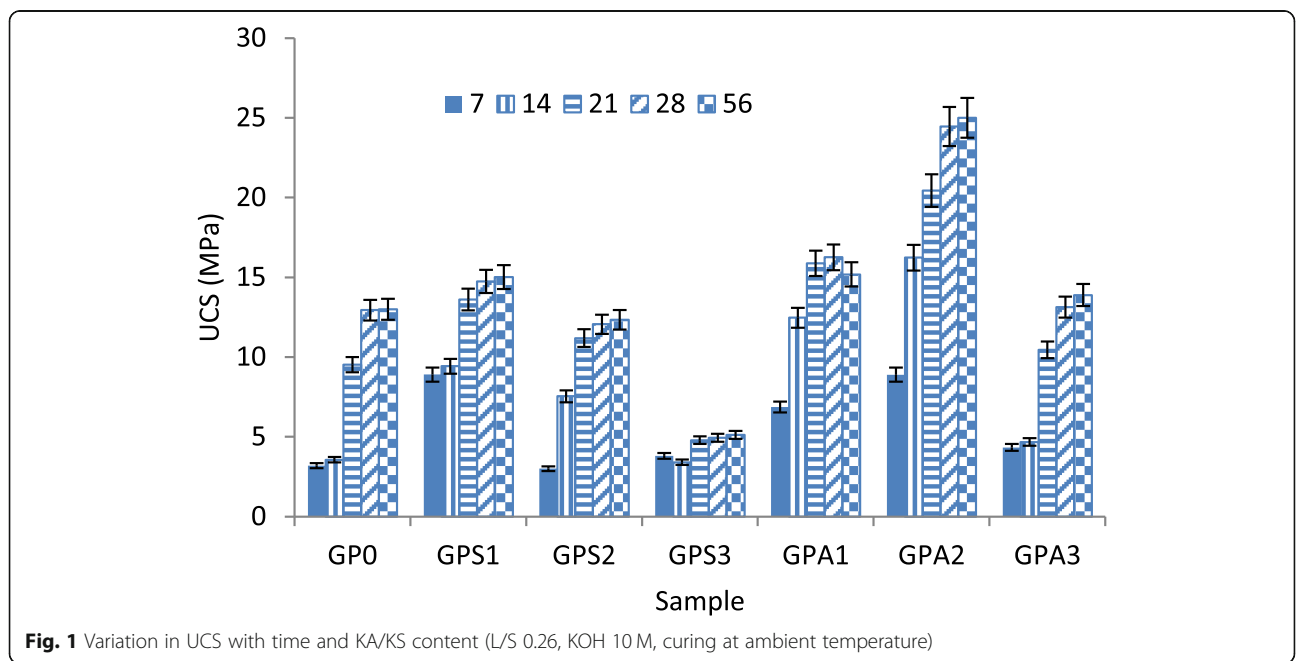


Fig. 1 Variation in UCS with time and KA/KS content (L/S 0.26, KOH 10 M, curing at ambient temperature)

(Sample GPA2) and KS:KOH 1.5 (Sample GPA3). The pastes were made by mixing the respective solutions with crushed FeCr slag at a L/S ratio of 0.26 and mixed in a machine to form a uniform paste. The pastes were then poured into 50 × 50 × 50 mm mould and allowed to harden at room temperature for 1 d. After 1 d, the hardened pastes were demoulded and cured at ambient temperatures for 7, 14, 21, 28 and 56 d. The UCS was determined at the end of each curing period, with the crushed sample subsequently subjected XRD, FTIR and leachability tests.

Leachability tests

TCLP test was carried out as per USEPA method 1311 [20] using FeCr slag and the respective geopolymer samples. A modified static USEPA 1311 was used to determine the long term leaching characteristic of the geopolymers. The cured geopolymers without being crushed were placed in a column and completely covered with an extraction buffer of acetic acid and sodium acetate (pH 4.93 ± 0.05). The static extraction was left for 30 d. At the end of the 30 d, the extraction buffer was withdrawn completely before being acidified with nitric acid and subsequent metal analysis on the AAS. A

fresh extraction buffer was also added to the soaked geopolymer. This routine was repeated for 12 months.

Open porosity, water absorption and wet UCS

The modified ASTM C373-14a [21] method was used to determine open porosity. The cured geopolymer was soaked in water for 24 h. After 24 h, the geopolymers were removed from the water and visible water on the geopolymer was wiped using a soft cloth. The wet geopolymers were weighed within 5 min of being removed from water. Open porosity, *f*, was then calculated as:

$$f = \frac{W_s - W_d}{Va} \tag{1}$$

where *W_s* is the mass of the soaked geopolymer, *W_d* was the mass of the dry geopolymer, *V* was the volume of the geopolymer and *a* was the density of water. Water absorption was calculated as the difference in weight between the dry geopolymer and the soaked geopolymer. Wet UCS was conducted as per ASTM D5102 [19] on the soaked geopolymer. A modified ASTM D559 [22] was used to determine the variation of UCS with alternate wet and dry cycles.

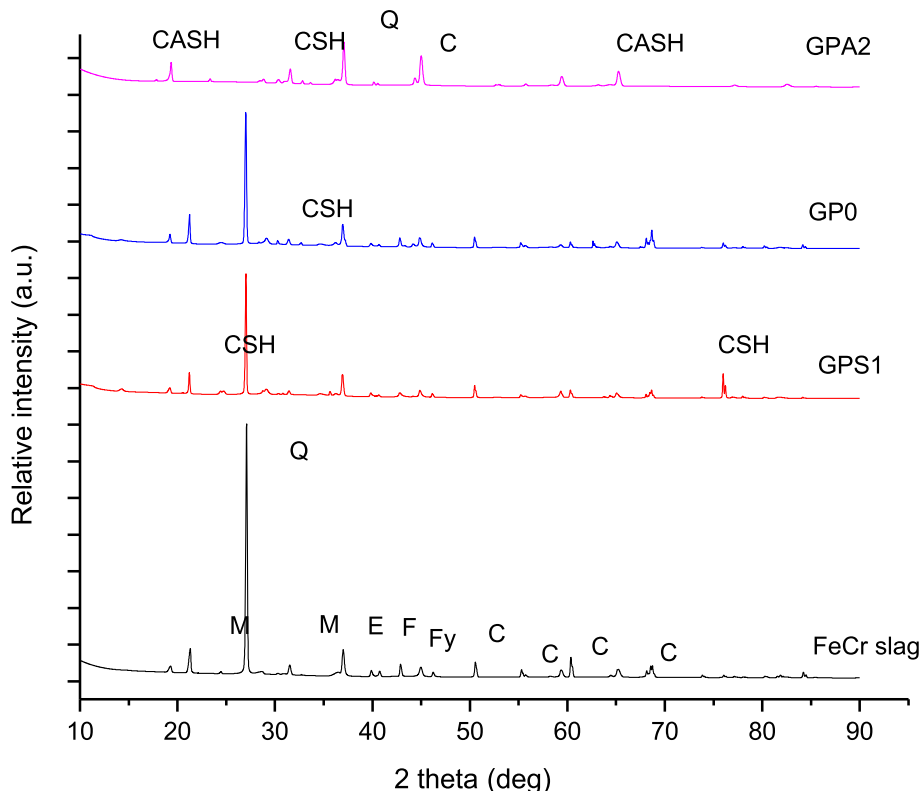


Fig. 2 XRD diffractogram of FeCr slag and various geopolymers (L/S 0.26, KOH 10 M, curing at ambient temperature, curing time 28 d) M = Magnesiochromite, F = Fosterite, Fy = Fayalite, C = Chromite, E = enstatite

Statistical analysis

The reported results are the average of three test samples. Statistical analysis was achieved using ANOVA in Excel. The error bars were at 95% confidence interval.

Results and discussion

Effect of KOH concentration and L/S ratio on the UCS of the geopolymer

At a fixed concentration of KOH, there was an increase in the UCS of the obtained geopolymers with an increase in L/S up to 0.26 (Table 2). A further increase in L/S beyond 0.26 resulted in a decrease in UCS. The increase in UCS was due to increase in the availability of OH⁻ ions which are required for the dissolution of Si, Ca and Al. The increase L/S ratio also resulted in uniform mixing of FeCr slag allowing for uniform dissolution of reacting species. The decrease in UCS with an L/S greater than 0.26 may be due to excess liquid which would not be utilized during geopolymerisation and would be lost during curing period leaving voids in the monolith thereby creating a weak structure. The excess liquid also made the hardening process difficult as evidenced by the design mix having an L/S of 0.30 which did not harden after 56 d of curing. At a fixed L/S, there was an increase in UCS from 5 to 10 M KOH, followed by a decrease in UCS at 15 M KOH. The initial increase

in UCS was due to increase in available OH⁻ ions whereas the decrease at 15 M may be due to excess K⁺ ions in the design mix which then failed to charge balance the mixture [23]. The design mix which gave the highest UCS was L/S 0.26, KOH concentration of 10 M (Table 2). The resultant geopolymer from this mix was the labelled as GP0. The strength gain (solidification) of FeCr slag was due to the formation of calcium silicate hydrate phases after geopolymerisation as seen in Fig. 2 (geopolymer GP0).

Effect of curing time and KA/KS on the UCS of the geopolymers

There was an increase in the UCS with time for all geopolymers (Fig. 1). The increase was statistically significant up to 28 d for the aluminate activated geopolymers (GPA) and the pure FeCr geopolymer (GP0) whereas the increase was statistically significant up to 21 d for the silicate activated geopolymer (GPS). There was no statistical significant difference in UCS between 28 and 56 d for all geopolymers. GPS geopolymers may have attained UCS at a faster rate because of the availability of soluble Si to participate in the geopolymerisation. GP0 and GPA geopolymers were slower in that the dissolution of Si from FeCr played a critical role in the formation of the geopolymer. On the average the GPA had a higher UCS

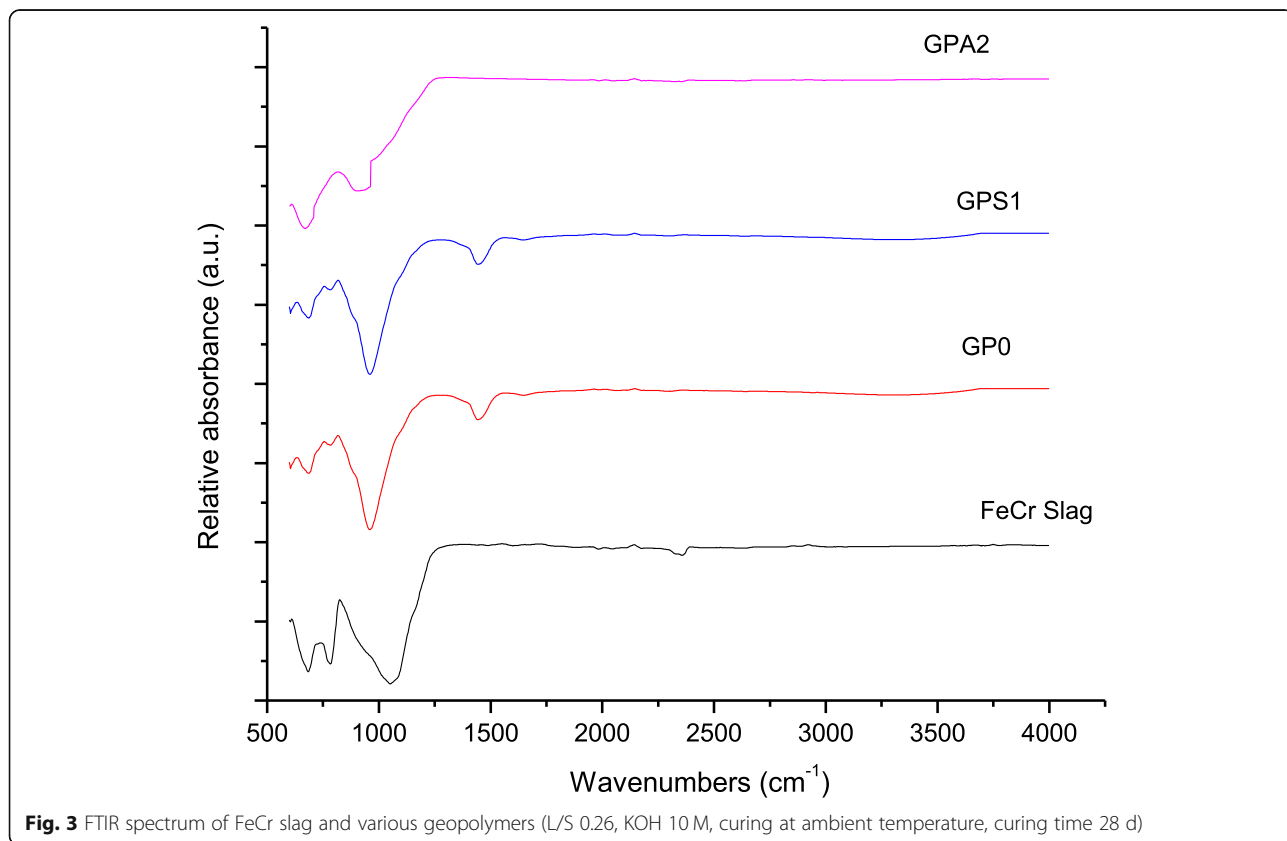


Fig. 3 FTIR spectrum of FeCr slag and various geopolymers (L/S 0.26, KOH 10 M, curing at ambient temperature, curing time 28 d)

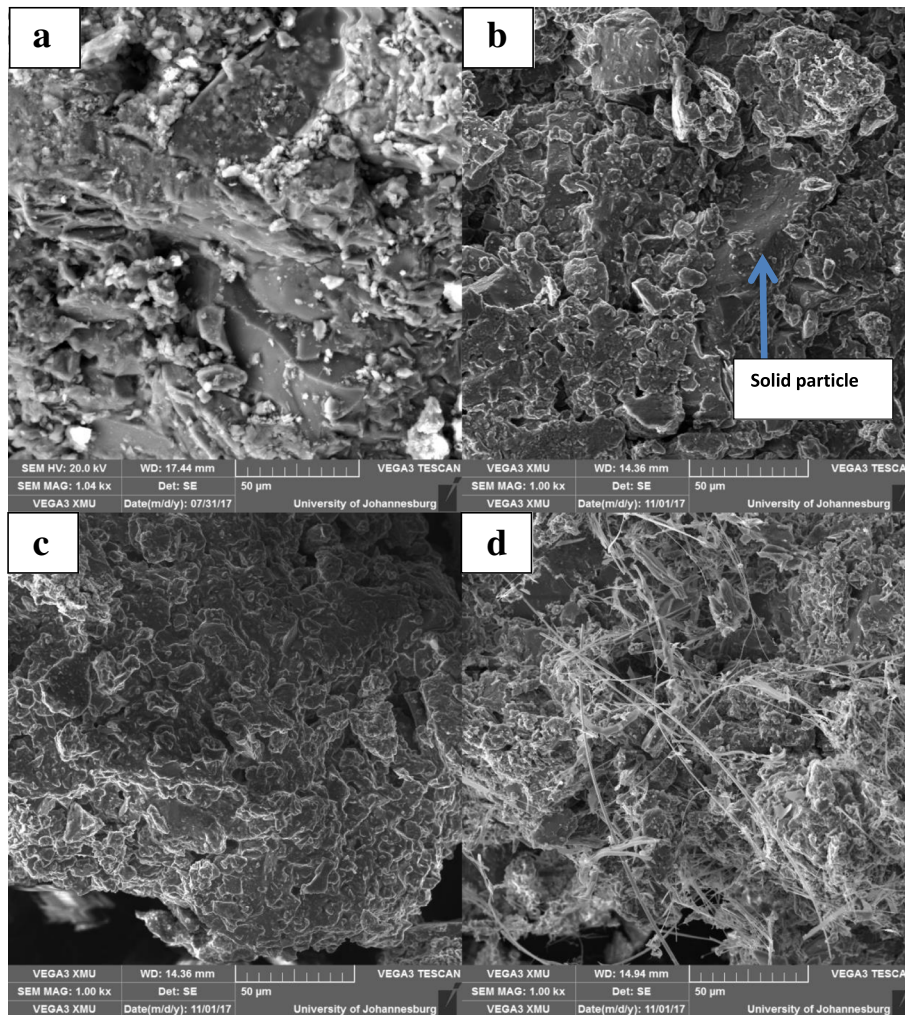


Fig. 4 SEM micrographs of FeCr slag (a), GP0 (b), GPS1 (c) and GPA2 (d) (L/S 0.26, KOH 10 M, curing at ambient temperature, curing time 28 d)

as compared to GP0 and GPS. This was due to that the aluminate activation resulted in the formation of calcium silicate hydrate and calcium aluminate silicate hydrate in the geopolymers whereas silicate activation resulted in the formation of calcium silicate hydrate only. It has been shown that the right balance between Si and Al in the precursors or activating materials is important to get a high UCS [24]. This is because the two have to dissolve and then rearrange into a three dimensional structure. The highest UCS was thus obtained from GPA 2 (Fig. 1) which had a Si/Al ratio of 1.92. This ratio falls within the range of Si/Al (1–3) that has been shown to give the maximum UCS for a number of precursors [25–27]. GP0 had a Si/Al ratio of 4.33 and the GPS geopolymers had a Si/Al greater than 4.33.

Spectroscopic analysis

The major mineral phases were Quartz, Fayalite, Magnesiochromite, Chromite, Fosterite and Enstatite. XRD

Table 3 TCLP analysis of FeCr slag and the geopolymers (L/S 0.26, KOH 10 M, curing at ambient temperature, curing time 28 d)

	Fe (ppm)	Zn (ppm)	Mn (ppm)	Ni (ppm)	Cr (ppm)
FeCr Slag	550	10.4	20.5	4.34	320
GP0	26	0.31	0.26	0.18	11
GPS1	4	0.32	0.27	0.21	4.5
GPS2	27	0.38	0.38	0.22	11
GPS3	32	0.44	0.22	0.14	26
GPA1	13	0.38	0.24	0.28	1.6
GPA2	3	0.23	0.24	0.15	0.9
GPA3	16	0.37	0.26	0.29	4.9
Allowable Limits	5	4	10	0.4	5

Table 4 Long term leachability (Total metal release over 12 months) (L/S 0.26, KOH 10 M, curing at ambient temperature, curing time 28 d)

Sample	Fe (ppm)	Zn (ppm)	Mn (ppm)	Ni (ppm)	Cr (ppm)
GPO	45.7	1.23	1.78	3.76	15.7
GPS1	7.45	1.33	1.44	1.23	7.54
GPA2	1.34	1.24	0.88	0.88	1.21

analysis of GPO and GPS1 showed a reduction in the intensity of all minerals in the XRD diffractogram of FeCr slag (Fig. 2). The most significant was the reduction in the intensity of the quartz peak. This may be evidence of the reduction in crystallinity of the precursor. The reduction in the intensity of the quartz peak was also evidence of the participation of quartz in the dissolution reactions. This phenomenon of the dissolution of crystalline species has also been reported in literature [24]. GPO and GPS1 showed the formation Calcium Silicate Hydrate (CSH) around 20° and 78° [28, 29]. The formation of CSH was responsible for the gain in strength. The GPS1 geopolymer had a higher UCS than the GPO geopolymer due to the presence of more CSH peaks than the GPO geopolymer (Fig. 2). The GPA2 geopolymer had a completely different XRD diffractogram from GPO and GPS1 (Fig. 2). The GPA2 had a complete shift of the quartz peak from about 24° to about 34°. This represented a complete restructuring of the mineral as shown in the FTIR spectrum (Fig. 3). The XRD diffractogram of GPA2 was also elevated from 15° to 32°, which showed that there was introduction of the amorphous structure into the geopolymer. The GPA2 geopolymer also contained Calcium Aluminate Silicate Hydrate (CASH) in addition to CSH [30]. The additional CASH was a result of the increase in the aluminate available in the activator which also led to an increase in the strength of GPA2 in comparison to GPS1 and GPO (Fig. 2).

FTIR analysis

FeCr slag is characterised by bands around 683 and 783 cm^{-1} , which are typical of metal oxides and spinels of magnesiochromite [31] (Fig. 3). The band around 1050 cm^{-1} is typical of Si-O vibrations [32]. The band around 2356 cm^{-1} may be assigned to hydroxyl stretching of CaOH/CaO [33]. There was a shift to lower wavenumber of the main Si-O vibrations peaks for all geopolymers as compared to the FeCr slag. The main peak for FeCr slag

was at 1050, GPO at 998, GPS at 962, and GPA2 at 906.3 cm^{-1} . This showed that there was a direct link in the reduction of crystallinity with an increase in the UCS of the geopolymers. The building units of materials can be written as SiQ^n units. The value of n represents the crystallinity of the material. The SiQ^n units are usually found in the 850–1200 cm^{-1} where $n = 4, 3, 2, 1, 0$ when absorption is centred at around 1200, 1100, 950, 900, and 850 cm^{-1} , respectively [25]. The n value changed from 3 for FeCr slag, to 2 for GPO and GPS1 and 1 for GPA2. The lower the value of n , the less crystalline the material [25]. This was also supported by the XRD analysis (Fig. 2). The reduction in wavenumbers was due to the incorporation of Al into the Si-O bonds. The larger the incorporation of Al, the larger the shift as seen with the GPA2 geopolymer which had KA in the activation liquid. The aggressive alkaline nature of the geopolymerisation process resulted in the reorganisation of the spinel bonds around 683 and 783 cm^{-1} , which may be due to incorporation of CASH/CSH into the structure. There was also the introduction of peaks around 1450 cm^{-1} for GPO and GPS1. These peaks are resolved as carbonates peaks which may have been caused by the absorption of atmospheric CO_2 during pasting and curing. The GPA2 had a significant reduction in the intensity of the Si-O bond accompanied also with the peak losing its sharpness as compared to FeCr slag, GPO and GPS1. This may have been due to the re-orientation of bonds as seen in the obtaining XRD analysis (Fig. 2).

SEM

FeCr slag consists of large particles with very fine particles on the surface (Fig. 4a), indicating the crystallinity of the slag. Geopolymerisation resulted in the breaking up of the large particles into smaller particles. This was due to the dissolution of minerals under the alkaline conditions allowing for more packing of particles during curing leading to an increase in the UCS. The GPO had visible large particles which may indicate incomplete geopolymerisation (Fig. 4b); these particles were not visible in GPS1 and GPA2. GPA2 also had rod like particles after geopolymerisation (Fig. 4d). It has also been shown that a decrease in particle regularity can lead to increase in the compressibility of particles leading to a higher UCS [34].

TCLP

All geopolymers were effective in the immobilisation of Zn, Mn and Ni (Table 3). GPS1 and GPA2 were also

Table 5 Metal release rates (L/S 0.26, KOH 10 M, curing at ambient temperature, curing time 28 d)

Sample	Fe (mg m^{-2})	Zn (mg m^{-2})	Mn (mg m^{-2})	Ni (mg m^{-2})	Cr (mg m^{-2})
GPO	3043	82	119	251	1044
GPS1	497	89	96	82	503
GPA2	89	83	59	59	81

Table 6 Geopolymer Physical Properties (L/S 0.26, KOH 10 M, curing at ambient temperature, curing time 28 d)

Geopolymer	GP0	GPS1	GPA2
Mass of geopolymer (g)	350.46	360.64	362.27
Mass of cast after 24 h soak (kg)	399.45	390.35	385.13
Open porosity	0.39	0.24	0.18
UCS (MPa)	12.9	14.7	24.5
UCS (MPa) after 24 h soak	3.9	8.7	19.9
Water absorption %	14.0	8.2	6.3

effective in the immobilisation of Fe and Cr although the Fe and Cr immobilisation by GPS1 was within the error limits of the allowable limits. Although the XRD analysis did not reveal any structures with the metals in question, immobilisation/solidification was due to the incorporation of the metals into the CASH/CSH (Fig. 2) [35]. The highest immobilisation was in GPA2 where there was over 97% reduction in metal leachability with over 99.7% reduction in Cr leachability. The reduction in metal solubilities was due to either formation of insoluble metal hydroxides or incorporation of metal into CASH/CSH [36]. Dilution had minimal effects as the dilution was less than 30% yet solubilities were reduced by over 85%.

The release of metals into the environment for any material is a barrier to its use. GPA2 geopolymer had the lowest metal release after 12 months of static TCLP (Table 4). This shows that the GPA2 geopolymer can be used safely without major environmental contamination. The total metal release for GP0 and GPS1 was above the allowable limits and hence they are not suitable for long term use. This shows that UCS alone cannot be used as a criterion for the suitability of a material to be used in the construction industry.

Metal release rates can also be used to determine the safety to use a particular material in the construction industry [5]. The 12 months metal release rates for GPA2 were well below allowable limits and therefore suitable to be used in the construction industry (Table 5). This therefore means where GPA2 is used there will be no significant Fe, Cr, Zn, Mn and Ni pollution.

Physical properties of the geopolymers

The physical properties of a geopolymer determine where it can be used in the construction industry. The GPA2 satisfies the minimum conditions for use as building brick under severe weathering conditions ASTM C62–10 [37] and for a pedestrian and light traffic paving brick under medium weathering ASTM C902–07 [38] (Table 6). The effect of soaking the geopolymer in water for 24 h resulted in a UCS loss of 70, 41 and 19% for GP0, GPS1 and GPA2, respectively.

The resistance to strength changes with wet and dry cycles can be used as a measure of materials’ durability. After 10 cycles, the GPO geopolymer had a UCS loss of 91%, GPS1 UCS loss of 72% whilst the GPA2 had a loss of 42% (Fig. 5). It is worth mentioning that the GPA2 had the highest resistance to wet and dry cycles and therefore could withstand variations in extreme weather of alternate droughts and floods. GPA2 compared well with the few known studies regarding FeCr slag geopolymers [15, 16]. The previous studies had geopolymers with a UCS ranging from 13 to 35 MPa [15, 16]. UCS was the only meaningful comparison which could be done as the other studies did not include metal leachability and long term stability of the FeCr slag geopolymers.

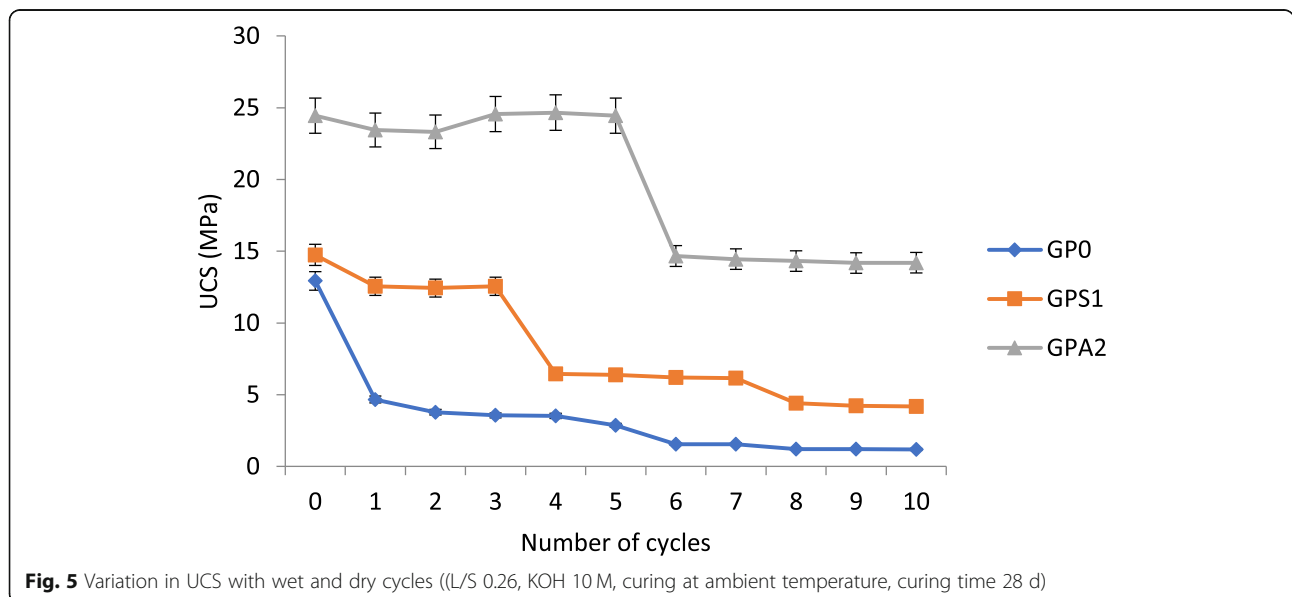


Fig. 5 Variation in UCS with wet and dry cycles (L/S 0.26, KOH 10 M, curing at ambient temperature, curing time 28 d)

Conclusions

FeCr slag can be used as a precursor for the synthesis of geopolymers. The quality of the geopolymer depends on the activating solutions, KOH concentration and the L/S. Aluminate activation of the FeCr slag yields a more competent geopolymer as compared to silicate activation. Geopolymerisation leads to reduction in metal leachability through the possible incorporation of metals in the CSH/CASH phases in the geopolymer which are also responsible for the increase in the UCS in the synthesised geopolymers. A 28-d ambient temperature curing is the optimum curing time for the GPA, GPS and pure FeCr. The GPA can be used for light traffic pavement construction which would result in high volume utilization of the slag. The possible environmental pollution with continued use is minimal for the GPA as compared to the GPS and pure FeCr slag geopolymers.

Acknowledgements

The author would like also to thank the University of Johannesburg for granting the Global Excellence Stature research fund (201323467) to the author.

Author's contribution

The author carried out laboratory work and wrote the article. The author read and approved the final manuscript.

Funding

The author's research is funded by the University of Johannesburg under the Global Excellence Stature (GES) 201323467.

Availability of data and materials

The datasets supporting the conclusions of this article are included within the article.

Competing interests

The author declares that he has no competing interests.

Received: 29 January 2019 Accepted: 8 July 2019

Published online: 01 August 2019

References

- Richard P. Overview of the global chrome market. In: Proceedings of INDINOX Stainless Steel Conference. Ahmedabad: International Chromium Development Association; 2015.
- Sahu N, Biswas A, Kapure GU. A short review on utilization of ferrochromium slag. *Min Proc Ext Met Rev*. 2016;37:211–9.
- Beukes JP, Guest RN. Cr(VI) generation during milling. *Miner Eng*. 2001;14:423–6.
- Beukes JP, Pienaar JJ, Lachmann G, Giesecke EW. The reduction of hexavalent chromium by sulphite in wastewater. *Water SA*. 1999;25:363–70.
- Panda CR, Mishra KK, Panda KC, Nayak BD, Nayak BB. Environmental and technical assessment of ferrochrome slag as concrete aggregate material. *Constr Build Mater*. 2013;49:262–71.
- Erdem M, Altundogan HS, Turan MD, Tumen F. Hexavalent chromium removal by ferrochromium slag. *J Hazard Mater*. 2005;126:176–82.
- DWAF. Waste management series. Minimum requirements for the handling, classification and disposal of hazardous waste. 2nd ed. Pretoria: Department of Water Affairs & Forestry; 1998.
- Wang S, Vipulanadan C. Solidification/stabilization of Cr(VI) with cement: leachability and XRD analyses. *Cem Concr Res*. 2000;30:385–9.
- Olmo IF, Chacon E, Irabien A. Influence of lead, zinc, iron (III) and chromium (III) oxides on the setting time and strength development of Portland cement. *Cem Concr Res*. 2001;31:1213–9.
- Lind BB, Fallman AM, Larsson LB. Environmental impact of ferrochrome slag in road construction. *Waste Manag*. 2001;21:255–64.
- Zelic J. Properties of concrete pavements prepared with ferrochromium slag as concrete aggregate. *Cem Concr Res*. 2005;35:2340–9.
- Gencel O, Sutcu M, Erdogmus E, Koc V, Cay VV, Gok MS. Properties of bricks with waste ferrochromium slag and zeolite. *J Clean Prod*. 2013;59:111–9.
- Chen JY, Wang YH, Zhou S, Lei XR. Reduction/immobilization processes of hexavalent chromium using metakaolin-based geopolymer. *J Environ Chem Eng*. 2017;5:373–80.
- Provis JL. Alkali-activated materials. *Cem Concr Res*. 2018;114:40–8.
- Karakoc MB, Turkmen I, Maras MM, Kantarci F, Demirboga R, Toprak MU. Mechanical properties and setting time of ferrochrome slag based geopolymer paste and mortar. *Constr Build Mater*. 2014;72:283–92.
- Nath SK. Geopolymerization behavior of ferrochrome slag and fly ash blends. *Constr Build Mater*. 2018;181:487–94.
- DWAF. South African water quality guideline. 2nd ed. Pretoria: Department of Water Affairs & Forestry; 1996.
- ASTM. Standard Practice for Making and Curing Concrete Test Specimens in the Laboratory (ASTM C192). West Conshohocken: American Society for Testing and Materials International; 2016.
- ASTM. Standard Test Methods for Unconfined Compressive Strength of Compacted Soil-Lime Mixtures (ASTM D5102) (withdrawn 2018). West Conshohocken: American Society for Testing and Materials International; 2009.
- USEPA. Toxicity Characteristic Leaching Procedure. Washington, DC: US Environmental Protection Agency; 1992.
- ASTM. Standard Test Method for Water Absorption, Bulk Density, Apparent Porosity and Apparent Specific Gravity of Fired Whiteware Products, Ceramic Tiles and Glass Tiles (ASTM C373). West Conshohocken: American Society for Testing and Materials International; 2014.
- ASTM. Standard Test Methods for Wetting and Drying Compacted Soil-Cement Mixtures (ASTM D559). West Conshohocken: American Society for Testing and Materials International; 2015.
- Khale D, Chaudhary R. Mechanism of geopolymerization and factors influencing its development: a review. *J Mater Sci*. 2007;42:729–46.
- Ren X, Zhang LY, Ramey D, Waterman B, Ormsby S. Utilization of aluminum sludge (AS) to enhance mine tailings-based geopolymer. *J Mater Sci*. 2015;50:1370–81.
- Zhang LY, Ahmari S, Zhang JH. Synthesis and characterization of fly ash modified mine tailings-based geopolymers. *Constr Build Mater*. 2011;25:3773–81.
- Cheng TW, Chiu JP. Fire-resistant geopolymer produced by granulated blast furnace slag. *Miner Eng*. 2003;16:205–10.
- Stevenson M, Sagoe-Crentsil K. Relationships between composition, structure and strength of inorganic polymers. Part I - Metakaolin-derived inorganic polymers. *J Mater Sci*. 2005;40:2023–36.
- Aliabdo AA, Abd-Elmoaty AEM, Hassan HH. Utilization of crushed clay brick in concrete industry. *Alexandria Eng J*. 2014;53:151–68.
- Kontoleonos F, Tsakiridis P, Marinos A, Katsiotis N, Kaloidas V, Katsioti M. Dry-grinded ultrafine cements hydration. Physicochemical and microstructural characterization. *Mater Res-Lbero-Am J*. 2013;16:404–16.
- Torres-Luque M, Osma JF, Sanchez-Silva M, Bastidas-Arteaga E, Schoefs F. Chloridetect: commercial calcium aluminate based conductimetric sensor for chloride presence detection. *Sensors-Basel*. 2017;17:1–19.
- Allen GC, Paul M. Chemical characterization of transition metal spinel-type oxides by infrared spectroscopy. *Appl Spectrosc*. 1995;49:451–8.
- Wilson MJ, editor. Clay mineralogy: spectroscopic and chemical determinative methods. London: Chapman & Hall; 1994.
- Navarro C, Diaz M, Villa-Garcia MA. Physico-chemical characterization of steel slag. Study of its behavior under simulated environmental conditions. *Environ Sci Technol*. 2010;44:5383–8.
- Cho GC, Dodds J, Santamarina JC. Particle shape effects on packing density, stiffness, and strength: natural and crushed sands. *J Geotech Geoenviron*. 2006;132:591–602.
- Huang X, Zhuang RL, Muhammad F, Yu L, Shiau YC, Li DW. Solidification/stabilization of chromite ore processing residue using alkali-activated composite cementitious materials. *Chemosphere*. 2017;168:300–8.
- Lasheen MR, Ashmawy AM, Ibrahim HS, Moniem SMA. Immobilization technologies for the management of hazardous industrial waste using granite waste (case study). *Korean J Chem Eng*. 2016;33:914–21.
- ASTM. Standard Specification for Building Brick (Solid Masonry Units Made from Clay or Shale) (ASTM C62). West Conshohocken: American Society for Testing and Materials International; 2010.

38. ASTM. Standard Specification for Pedestrian and Light Traffic Paving Brick (ASTM C902). West Conshohocken: American Society for Testing and Materials International; 2007.

Publisher's Note

Springer Nature remains neutral with regard to jurisdictional claims in published maps and institutional affiliations.

Ready to submit your research? Choose BMC and benefit from:

- fast, convenient online submission
- thorough peer review by experienced researchers in your field
- rapid publication on acceptance
- support for research data, including large and complex data types
- gold Open Access which fosters wider collaboration and increased citations
- maximum visibility for your research: over 100M website views per year

At BMC, research is always in progress.

Learn more biomedcentral.com/submissions

